

Received: 20 September 2007,

Revised: 3 April 2008,

Accepted: 4 April 2008,

Published online in Wiley InterScience: 27 May 2008

(www.interscience.wiley.com) DOI 10.1002/poc.1386

Changes of electron density in the OHN hydrogen bond upon proton transfer in complexes of phenols with trimethylamine: DFT study

Emilia Kwiatkowska^a and Irena Majerz^{a*}

The intermolecular hydrogen bonds in phenol-trimethylamine complexes were investigated by Bader Atom in Molecules (AIM) theory. The AIM parameters of the bond critical points (BCPs) of the O···H, N···H, and CO bonds as well as those of the phenol ring critical point (RCP) were analyzed as functions of the proton-transfer degree. Transfer of the proton from donor to acceptor changes not only the electron density of the hydrogen bridge, but also the electron cloud in the proton donor. The differences between the proton donors in relation to their pK_a values are seen in the systematic changes of the AIM parameters. Copyright © 2008 John Wiley & Sons, Ltd.

Supplementary electronic material for this paper is available in Wiley InterScience at <http://www.mrw.interscience.wiley.com/suppmat/0894-3230/suppmat/>

Keywords: hydrogen bonding; AIM analysis; phenol–amine complex

INTRODUCTION

The hydrogen bond has been intensively investigated from many years using both experimental and theoretical methods, but many phenomena connected with proton transfer from donor to acceptor still need clarification. One of the systems which have been very well investigated experimentally are complexes of phenols with tertiary amines in which a single OHN hydrogen bond is formed and where there is a possibility of almost continuous control of the donor–acceptor properties of the interacting components so that the proton in the hydrogen bridge can be gradually shifted from donor to acceptor. Structural measurements^[1] and *ab initio* calculations of the structure^[2–4] show that the proton-transfer process causes significant modification of the geometrical parameters of the hydrogen bridge, moderate changes in the structure of the proton donor, and small changes in the structure of the proton acceptor. Relationships between the structural parameters of the hydrogen bridges have been investigated for many years.^[5–7] Rich experimental material, including dipole moment measurements,^[8–10] NMR,^[11–13] NQR,^[14–16] IR,^[17,18] and UV spectra,^[17,19,20] has also been gathered. The structural data as well as other experimental results suggest that proton transfer in the hydrogen bridge must be connected with a fundamental rearrangement of the electron cloud surrounding the bridge atoms.

The direct method of investigating electron density is X-ray measurement, which is able to show the electron cloud. Another method, equivalent to the experimental, is theoretical analysis with the method provided by the Atom in Molecules (AIM) theory developed by Bader,^[21] which not only provides a picture of the electron cloud, but also quantitative parameters describing the electron density at the critical points and in the atomic basins.

Many papers can be found in the literature devoted to AIM analysis of the hydrogen bond which correlate the electron density with geometric parameters of the hydrogen bridge. An exponential relationship between the electron density at BCPs and O···H distance was established for complexes of amine and phosphine oxides with different protondonors.^[22] The electron densities at the BCPs of O···H and N···H were analyzed for the gas phase and crystalline complexes^[23] and it was shown that the difference in the two bridges was determined by the heavy atom. The dependence of $\ln \rho$ on the distance was $\ln \rho = (1.682 \pm 0.060) - (2.829 \pm 0.048)d_{\text{OH/O}\cdots\text{H}}$ for OH and $\ln \rho = (1.611 \pm 0.014) - (2.677 \pm 0.010)d_{\text{NH/N}\cdots\text{H}}$ for NH. Another AIM parameter which was used to characterize the difference in the N···H and O···H interactions was the distance at which the Laplacian of the electron density changes sign. For O···H this was 1.35 Å and for N···H 1.42 Å. Systematic analysis of the Laplacian versus N···H and O···H distance was also performed for the complexes of 4-methylimidazole and 4-methylimidazolium acetate, in which the hydrogen-bonded proton was shifted from the proton donor to a proton acceptor.^[24] The AIM method also makes an analysis of the energetic properties of the electrons at the critical points possible. The energetic properties of heteronuclear hydrogen bonds were systematically investigated for OHN. The values of the Laplacian, potential, kinetic, and total energy of the electrons at the BCPs of the O···H and N···H

* Correspondence to: I. Majerz, Faculty of Chemistry, University of Wrocław, Joliot-Curie 14, PL 50-383 Wrocław, Poland.
E-mails: maj@wchuwr.chem.uni.wroc.pl; majerz@yahoo.com

^a E. Kwiatkowska, I. Majerz
Faculty of Chemistry, University of Wrocław, Joliot-Curie 14, PL 50-383 Wrocław, Poland

bonds were used to classify the hydrogen bond interactions and discuss their covalent–noncovalent character.^[25] Positive values of the Laplacian indicate a noncovalent interaction, but more precise measures are the values of the potential (V) and kinetic energy (G). A $-G/V$ ratio greater than 1 indicates a noncovalent interaction. Values lower than 1 suggest that the interaction is partially covalent.

Despite many articles characterizing the AIM parameters of the hydrogen bond, the simplest model systems of phenols with tertiary amines have not been investigated with this method and there is still a need to analyze the simplest intermolecular complexes with typical hydrogen bonds and to describe the changes in electron density which takes place under the transfer of a proton from a proton donor to a proton acceptor. The purpose of the present paper is to investigate the changes in electron density in the model complexes with an OHN hydrogen bond, namely, complexes of phenols with trimethylamine.

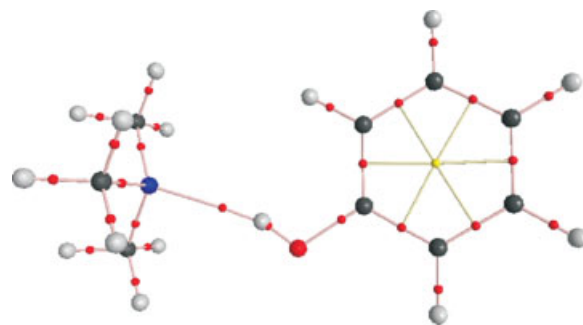
COMPUTATIONAL DETAILS

Complexes of trimethylamine with six phenols with different proton donor abilities (phenol, 4-nitrophenol, 2,6-dichlorophenol, 2,4-dinitrophenol, 2,6-dichloro-4-nitrophenol, and 2,4,6-trinitrophenol) were optimized at the DFT B3LYP/6-31G(d,p) level of calculation with the O···H distance kept fixed in steps of 0.1 Å from 0.8 to 2.1 Å and complete optimization of the other structural parameters. According to ref.,^[26,27] the DFT B3LYP/6-31G (d, p) method is known to be sufficient for describing the structures of complexes with hydrogen bonds. To check how the optimization method influences the geometry of the equilibrium structure, the optimization of phenol–trimethylamine complexes was also performed at the MP2/6-311++G** level. The calculations were performed with the Gaussian 03 program.^[28]

The wave function evaluated for each O···H distance was used as the input to the AIM2000 program,^[29] with all the default options. The integration of atomic properties over atomic basins was performed in natural coordinates, with a tolerance of 0.001 a.u. per integration step. The degree of proton transfer (X_{PT}) was calculated using the method described previously.^[30]

Previous investigations of the structural dependencies in phenol–tertiary amine upon shifting of the proton in the hydrogen bond^[1–4,30] showed that the most sensitive to proton transfer are the geometrical parameters of the hydrogen bridge, also including the CO bond length in the phenol molecule. More limited geometry changes than in the case of the bridge geometry are also seen for the phenolate ring. For this reason the analysis of the AIM parameters will concentrate on the bridge O···H···N, and the phenol C1 atoms and the bond critical points (BCPs) located on the O···H, N···H, and CO bonds. The ring critical point (RCP) located in the center of the aromatic ring of the phenol will also be analyzed as potentially sensitive to hydrogen bond strength. In Scheme 1, the structure of the phenol–trimethylamine complex and all the BCPs and the phenol RCP are depicted.

As the analysis will concern the changes in the hydrogen bridge upon proton transfer, a very important question is choosing the parameter which can express the degree of proton transfer. The initial parameter used to predict the degree of proton transfer is ΔpK_a ($=pK_a(BH^+) - pK_a(AH)$). Although this parameter is defined for an aqueous solution, it is commonly used also for nonhydrous solutions, gas phase, and the solid state.



Scheme 1.

It was shown^[31] that the dependency of ΔpK_a on the degree of proton transfer is a sigmoidal curve, and for this reason ΔpK_a is not very convenient as a parameter in the relationships. The sensitivity of hydrogen bridge length to proton transfer allows using the O···H and CO bond lengths as a measure of the proton-transfer degree and hydrogen bond strength, but these bond lengths are also sensitive to the interaction of the proton with the substituents in the ortho position of the phenol. A very well-known relationship between proton-transfer degree and dipole moment^[8] suggests that the best parameter to express the degree of proton transfer is the X_{PT} evaluated from the dipole moments^[30] estimated from the equation describing the dependence of the squared dipole moment $\mu^2 = \mu_{PT}^2 X_{PT} + \mu_{HB}^2 (1 - X_{PT})$ which was obtained assuming the additivity of the molar polarizability of a molecule existing in two tautomeric forms: HB – molecular hydrogen bond and PT – hydrogen bond with proton transferred to the acceptor atom. The values of dipole moments were obtained for optimized structure in Gaussian calculations. The values of μ_{HB} and μ_{PT} were estimated from the sigmoid dependence of the calculated dipole moments on the O—H distance $d(OH)$ according to the equation^[8], $\mu = \mu_{HB} + (\mu_{PT} - \mu_{HB}) [K/(1 + K)]$ where K is the proton transfer equilibrium constants. The points at largest $d(OH)$ were gradually eliminated in the procedure of reaching the best coincidence of fitted and obtained from Gaussian calculations dipole moments.

RESULTS AND DISCUSSION

Analysis of the OHN hydrogen bridge

Character of the AIM parameters of the BCPs

The geometric parameters of the hydrogen bridge and the AIM parameters of the bond critical points of OH and NH are collected in Table 1 (Supplementary Material).

The most important parameters in AIM analysis are connected with the BCPs. According to the Bader theory, the existence of BCPs as well as the presence of bond paths linking two atoms is a necessary condition for the existence of a chemical bond. In the case of very weak hydrogen bonds, the value of the electron density at a BCP must be higher than 0.002 a.u., which was found to be the boundary value for the existence of a hydrogen bond.^[32] In all the analyzed complexes, the OHN hydrogen bond is relatively strong; therefore, even in the weakest complexes analyzed in this study the values of the electron density are significantly higher, so the existence of the interaction is unquestioned. With increase in X_{PT} , $\rho(r)_{OH}$ decreases and $\rho(r)_{NH}$ increases. Both dependencies are linear only in the region close

to an X_{PT} of about 0.5. It is characteristic that the value of the electron density of the $O \cdots H$ group changes in a range about three times wider than the density at the BCP of the $N \cdots H$ bond. The range of the changes is connected with the strength of the bond. The hydrogen bonds with participation of $O \cdots H$ groups are stronger than those with $N \cdots H$ groups. Because the values of the electron density at the BCP of the $O \cdots H$ bond decreases with proton transfer, it could be expected that the highest $\rho(r)_{OH}$ will be equal to the value characteristic for phenols. These values change from 0.3654 (a.u.) for phenol to 0.3286 (a.u.) for picric acid, so the value of the electron density for the free OH group not engaged in a hydrogen bond cannot be included in the relationship of the $O \cdots H$ which participates in the hydrogen bond. On the other hand, the values of electron density of $N \cdots H$ attain 0.3424 (a.u.), typical for an $N^+ \cdots H$ bond in the trimethylamine cation. It is characteristic that the electron density at both critical points of the OHN bridge does not yield a relationship common to all the phenols, but a specificity of the phenol is seen, especially for the $O \cdots H$ bond. The electron density is highest for picric acid and lowest for phenol. Also, the crossing point of the electron density relationships of $O \cdots H$ and $N \cdots H$ is not exactly at $X_{PT}=0.5$, but moves from the lowest values for phenol to the highest for picric acid. A detailed discussion of the crossing-point parameters needs a more precise determination of the electron density in the X_{PT} range around 0.5, but it is seen that it is related to the pK_a value of phenol.

The electron densities at the $O \cdots H$ and $N \cdots H$ BCPs as a function of the interaction distance for the phenol-trimethylamine complexes are compared in Fig. 1 with the electron densities published previously.^[22,23,25] The common relationships for $O \cdots H$ and $N \cdots H$ are independent of the components of the hydrogen bond complex, although a difference between the $O \cdots H$ and $N \cdots H$ interactions is seen in the range of the electron density. When the results in ref.^[23] are typical for strong hydrogen bonds and those in^[22] for weak OHO interactions, the results for the phenol-trimethylamine complexes cover a very broad range of interactions of different strength and allow us to generalize the linear relationship of $\ln \rho$ with the distance. For $O \cdots H$, this is $\ln \rho = -2.5634d_{OH/O \cdots H} + 1.3645$ and for $N \cdots H$ $\ln \rho = -2.4697d_{NH/N \cdots H} + 1.3919$. The results obtained in this study confirm the universal character of the exponential dependence of the electron density on the distance.

Figure 2 shows the relation of the Laplacian of the electron density at both BCPs of the OHN bridge, $\nabla^2 \rho(r)$. Analogously to the relation of the electron density, the values of the Laplacian of the $N \cdots H$ bond are a few times lower than for $O \cdots H$ and the relationships are separated for the particular phenols.

The sign of the Laplacian identifies the regions of space where the charge is locally depleted ($\nabla^2 \rho(r) > 0$) or concentrated ($\nabla^2 \rho(r) < 0$). The Laplacian of the electron density can be used to classify the interatomic interactions: the shared-shell interaction ($\nabla^2 \rho(r) < 0$) and the closed-shell interaction ($\nabla^2 \rho(r) > 0$). Typical hydrogen bonds and Van der Waals complexes are examples of the closed-shell type, while covalent and polar bonds represent the shared-shell interaction. The value of $\nabla^2 \rho(r)$ in the 0–1 (a. u.) range expresses the special character of the interaction, which is intermediate between closed-shell and shared-shell. The interaction belongs to the closed-shell type,^[33] but a local concentration of charge also takes place, so the interaction has a mixed character, with contributions of the shared-shell and closed-shell. In this range electron density of the system undergoes a fundamental rearrangement which the molecular

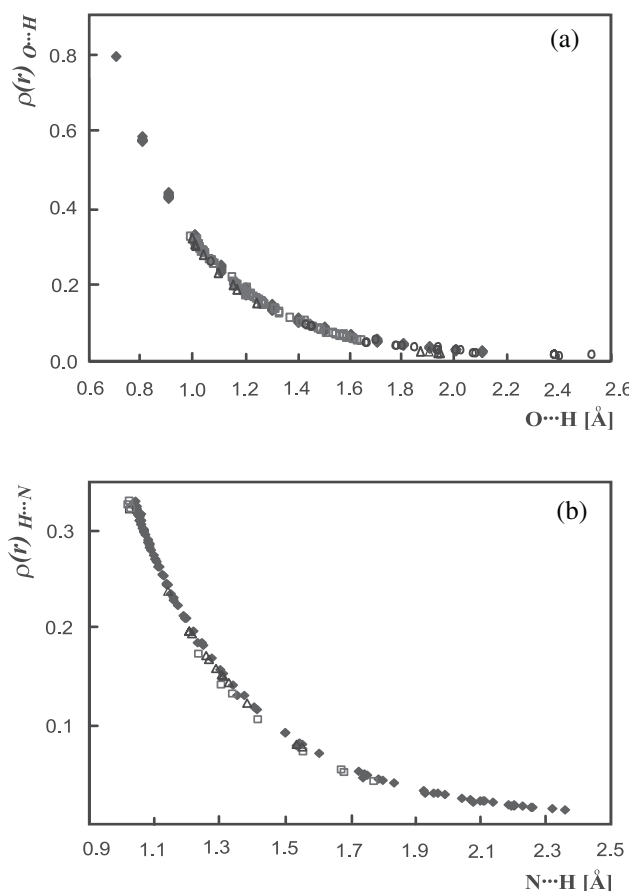


Figure 1. Electron density ($\rho(r)$) at the OH (a) and NH (b) bond critical points as a function of OH and NH distance, respectively. ◆ - this study, o, ref.^[22], □, △, ref.^[23]; □, △, ref.^[25] This figure is available in colour online at www.interscience.wiley.com/journal/poc

orbital is built. The closed-shell interaction region of the Laplacian of electron density can be divided into two regions depending on the values of potential ($V(r)_{CP}$) and kinetic ($G(r)_{CP}$) energies. For the $|V(r)_{CP}|/G(r)_{CP}$ ratio between 1 and 2 the hydrogen bond has partially covalent character. The value of $|V(r)_{CP}|/G(r)_{CP}$ ratio equal 1 is the boundary value at which the closed-shell interaction has partially covalent character.

For the analyzed compounds, the Laplacian of the electron density switches its sign at about 0.5 X_{PT} . Below this value the $O \cdots H$ bond is a closed-shell and the $N \cdots H$ bond a shared-shell interaction, while above 0.5 X_{PT} the characters of these bonds changes. The coordinates of the crossing point of the relationships for $O \cdots H$ and $N \cdots H$ are connected with the proton donor properties of the phenols. The minimum values of X_{PT} and $\nabla^2 \rho(r)$ at the crossing point of the OH and NH dependencies are lowest for phenol and highest for picric acid.

The eigenvalues of the Hessian matrix of the electron density ($\lambda_1, \lambda_2, \lambda_3$) are a source of information on the stability of the bond and its energetic properties. The ellipticity ($\varepsilon = (\lambda_1/\lambda_2) - 1$) at the BCP describes the deviation from centric concentration of the electron density at the BCP and provides a measure of the π character of a bond and its structural stability. In Fig. 3, the relations of the ellipticities at the BCPs characterizing the $O \cdots H$ and $N \cdots H$ bonds are compared. The difference between the

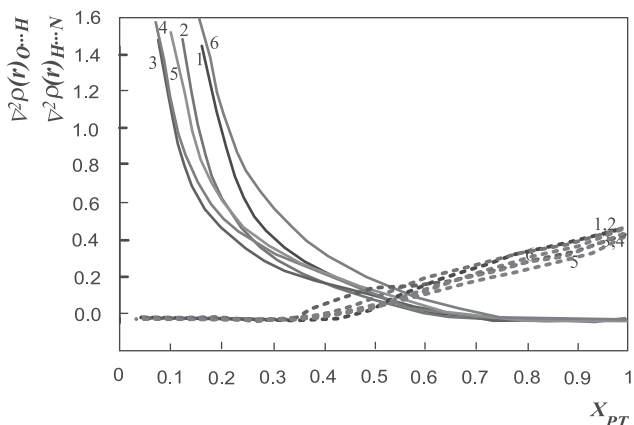


Figure 2. Laplacian of the electron density ($\nabla^2\rho(r)$) at the OH (solid line) and NH (broken line) bond critical points as a function of proton-transfer degree. The numbering of the phenols in all figures is according to their pK_a values: **1**, phenol ($pK_a = 9.99$); **2**, 4-nitrophenol (7.15); **3**, 2,6-dichlorophenol (6.08); **4**, 2,4-dinitrophenol (4.07), **5**, 2,6-dichloro-4-nitrophenol (3.68); and **6**, 2,4,6-trinitrophenol (picric acid) (0.42). This figure is available in colour online at www.interscience.wiley.com/journal/poc

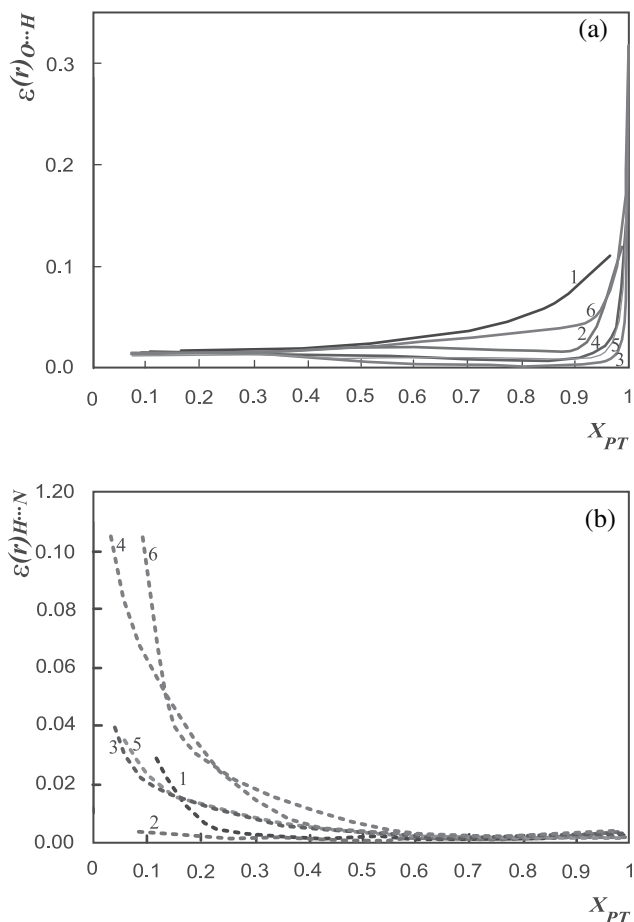


Figure 3. Ellipticity of the electron density at the OH (a) and NH (b) bond critical points as a function of proton-transfer degree (X_{PT}). This figure is available in colour online at www.interscience.wiley.com/journal/poc

relationships for $O \cdots H$ and $N \cdots H$ bonds is not only limited to higher values for $O \cdots H$, but is also seen in the slope of the lines. The curves for $O \cdots H$ change from 0, and above $X_{PT} = 0.5$ the ellipticity grows. For $N \cdots H$, the change in ellipticity decreases continuously from the high value characteristic for $X_{PT} = 0$. Above $X_{PT} = 0.5$, the ellipticity of the BCP between the N and H atoms is stabilized at the value close to 0, which means that the NH bond becomes stable. For $O \cdots H$, ε reaches the highest values at X_{PT} close to 1, which means that after shifting the proton to the acceptor, the $O \cdots H$ bond becomes unstable. In contrast, the $N \cdots H$ bond is unstable when the proton is located at the donor atom. In the relationships of ellipticity, the differences between the phenols used as proton donors are more clearly seen than in the relationships discussed above. The value of the ellipticity for both BCPs in the hydrogen bridge is the highest for picric acid and the lowest for phenol. The hydrogen bond is most unstable when is formed by the strongest phenol, so the proton can be easily moved between the donor and acceptor.

The eigenvalues of the Hessian matrix of the electron density can be used to calculate the potential and kinetic energy densities of the electrons at the critical points. The local kinetic electron energy density can be evaluated from the experimental electron density distribution according to the Abramov expression,^[34] which can be used in an approximated version for a closed-shell interaction.^[35] Comparison of the energy densities calculated by quantum chemical methods with those calculated using the approximate equations performed for large set of hydrogen-bonded complexes^[36] verifies the validity of the approximate equation. Both energy densities are related to the hydrogen bond distance. According to the equations presented in ref.,^[37] the kinetic energy density is $G = 15.3\lambda_3$ and the potential energy density $V = 35.1(\lambda_1 + \lambda_2)$. The potential energy of the electrons ($V(r)_{BCP}$) expresses the pressure exerted on the electrons at the BCP by other electrons. The kinetic energy ($G(r)_{BCP}$) reflects the mobility of the electrons at the BCP and the pressure exerted by the electrons at the BCP on other electrons. A comparison of both energies for the critical points located on the $O \cdots H$ and $N \cdots H$ bonds of the investigated OHN hydrogen-bonded complexes is shown in Fig. 4. Shifting the proton from the donor to the acceptor is connected with a decrease in the kinetic energy of the electrons at the BCP close to the proton donor and an increase in the kinetic energy at the BCP close to the acceptor. The potential energy changes in the opposite direction. When the electrons are less mobile, the energy exerted on them by other electrons is higher. The proton-transfer degree at which equalization of the kinetic and potential energies at the $O \cdots H$ and $N \cdots H$ BCPs takes place is about 0.5, but the values at the crossing point depend on the proton donor properties of the phenol. For a phenol with higher proton donor properties, the kinetic energy density at the $O \cdots H$ and $N \cdots H$ BCPs equals at higher X_{PT} values than for the phenol with lower proton donor properties. The mobility of the electrons in the $O \cdots H$ bond is highest when the proton-transfer degree is lowest, but for the free OH group in phenols the energy value is too low to be included in the relationship as the point with $X_{PT} = 0$. Transferring the proton from the donor to the acceptor is connected with changes in the mobility of the electrons at both critical points in the hydrogen bridge, and when the degree of proton transfer is 0.5, electron mobility at both BCPs is this same. Analogous energy equalization applies for the potential energy density. It is characteristic that the energies for the $O \cdots H$ bond change within a significantly broader range than for the $N \cdots H$ bond.

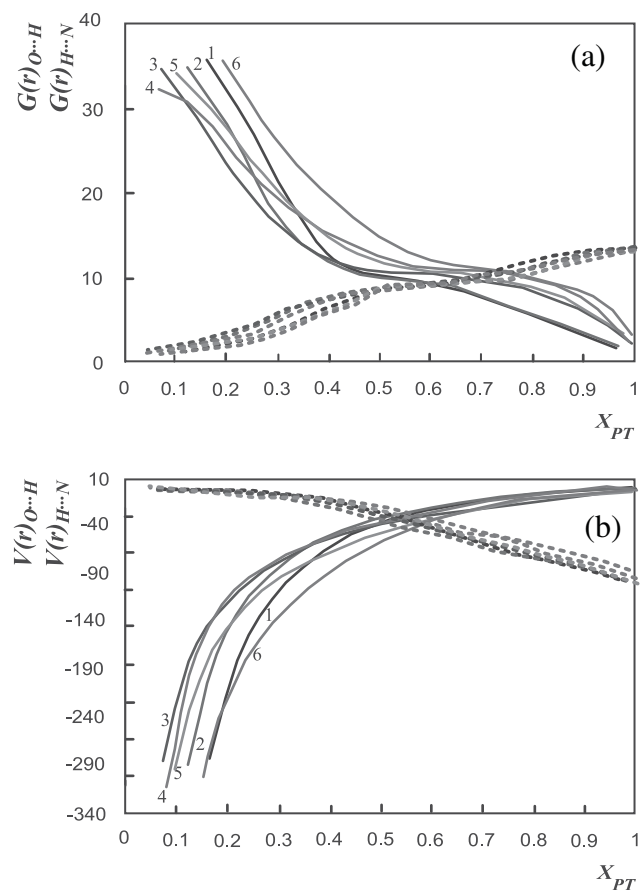


Figure 4. Kinetic energy density ($G(r)$) (a) and potential energy density ($V(r)$), (b) of electrons at the BCPs of OH (solid line) and NH (broken line) as functions of X_{PT} . This figure is available in colour online at www.interscience.wiley.com/journal/poc

Character of the atomic basins

AIM theory provides a partition of the molecular space into atomic basins associated with basins of zero local flux in the gradient vector field of the electron density and the basins correspond to topologically defined atoms. Such a precise partition of the molecule allows investigation of the electron density associated with a particular atom and discussion of the parameters concerning the atomic basins. It can be expected that in the proton-transfer process the atomic volumes of the proton, proton donor, and proton acceptor will change. The relationship of the atomic volumes of H, O, and N integrated over the 0.001 isosurface with X_{PT} is shown in Fig. 5. This dependency for the proton is similar to the sigmoidal curve typical for many experimental relationships. For X_{PT} around 0.5, this curve has a plateau and significantly increases for higher values of X_{PT} . This shape of the dependency of proton atomic volume on X_{PT} is characteristic for phenol without any substituent used as the proton donor. With increase in proton donor properties of phenol, these changes are less evident, and for picric acid the relationship between proton volume and X_{PT} seems to be a straight line with a low slope. The atomic volume of the donor oxygen atom grows linearly with X_{PT} , but this change is not very significant. The dependency on the proton donor properties is also seen in this relationship. The change is most evident for

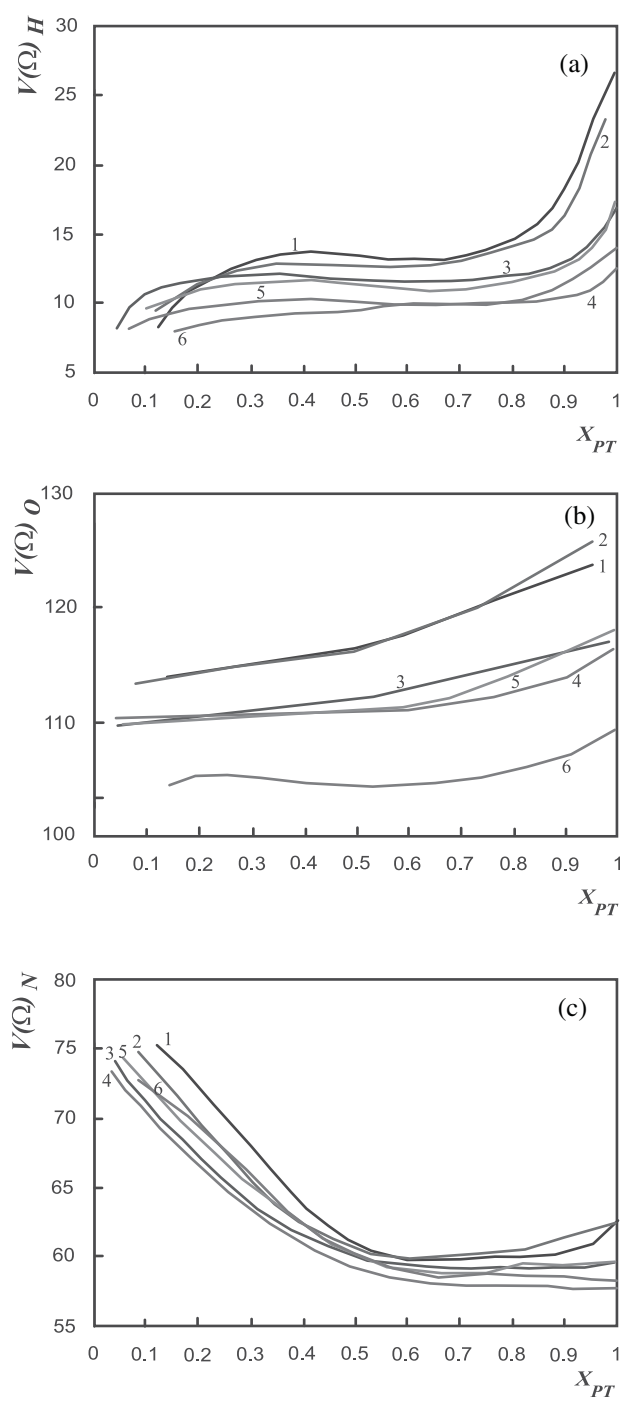


Figure 5. Relationship between the atomic volume integrated within the 0.001 isosurface of the atoms participating in the hydrogen bridge: H (a), O (b), and N (c), and the proton-transfer degree. The values of the atomic volumes of H, O in free phenols and O⁻ in the phenolate anions are respectively: phenol, 21.7748, 113.8061, 131.0570; 4-nitrophenol, 21.2046, 113.3520, 129.3497; 2,6-dichlorophenol, 18.9302, 111.6285, 111.1629; 2,6-dichloro-4-nitrophenol, 18.5680, 110.7825, 125.3135; 2,4-dinitrophenol, 11.9799, 113.3519, 123.5758; and picric acid, 11.2704, 106.2757, 118.7405. The atomic volumes of the H and N atoms in the trimethylammonium cation are 26.8351 and 61.7336, respectively. This figure is available in colour online at www.interscience.wiley.com/journal/poc

phenol and almost invisible for picric acid (the straight line for phenol: $V(\Omega)_0 = 8.4225 X_{PT} + 112.86$, $R^2 = 0.9169$, and for picric acid: $V(\Omega)_0 = 4.8019 X_{PT} + 103.04$, $R^2 = 0.69$). More significant is the decrease in the atomic volume of the proton acceptor atom. Shifting the proton to the nitrogen is connected with a decrease in the nitrogen atomic value, but only in the X_{PT} range of 0–0.5. Above this value, the atomic volume of nitrogen becomes constant.

Electron density integrated over the atomic volume within the 0.001 isosurface of the hydrogen bridge atoms (Fig. 6) is also sensitive to proton transfer. The relationship between the electron density in the atomic basin of the proton and the degree of proton transfer has an analogous shape to that of proton volume. The volume of the oxygen does not change significantly with proton transfer, but the electron density in the atomic basin is sensitive to proton transfer. In the atomic basin of the donor atom, the number of electrons decreases, reaching a minimum at about $X_{PT} = 0.5$, and then increases again. The shape of this relationship is connected with the pK_a value of the phenol and has the best shape for phenol without any substituent, and for picric acid it is close to a straight line. The electron density in the nitrogen atomic basin increases with proton shifting. This increase is very limited up to X_{PT} below 0.5, and above this value it is very significant.

All the relationships illustrate the mechanism which takes place in the proton-transfer process. The atomic basin of the proton enlarges when the proton moves to the acceptor by the value which the acceptor loses. Electrons from the donor atom are transmitted to the atomic basin of the acceptor, and when the proton is closer to the acceptor this process becomes more significant. This mechanism causes the changes in atomic volume and electron density in the atomic basin of the proton to be more complicated and their relationships with proton-transfer degree have complicated shapes.

Analysis of the BCP of the CO bond

Besides the OH and OH bonds, the proton-transfer process also influences the CO bond in the donor molecule, which changes in length from 1.36 Å typical for phenols^[38–42] to 1.26 Å characteristic for phenolates.^[43–45] For this reason it appeared interesting to investigate the AIM parameters of the CO bond. The geometric parameters of the CO bond and the AIM parameters of the electron density at the CO BCP are collected in Table 2 (Supplementary Materials). In Fig. 7 shows the relationship of electron density and kinetic and potential energy densities of the electrons at the BCP of the CO bond compared with the electron density at the BCPs of the OH and NH bonds, the value of the electron density as well as of the potential and kinetic energy densities for the CO bond change in a more limited scale. All these relationships are linear and the values for phenol can be used as a reference value for $X_{PT} = 0$. With the increase in the degree of proton transfer, the electron density at the BCP of the CO bond increases, the electrons become more mobile, and the pressure exerted by other electrons is lower. The CO distance is linearly related to X_{PT} ^[3,30] and therefore an equation common for all the investigated phenols can describe the electron density at the CO BCP versus the CO distance: $\rho(r)_{CO} = -0.8151d_{CO} + 1.3963$, $R^2 = 0.9939$. The relationship between electron density and the proton transfer degree reflects specific proton donor properties of the phenols which are not seen in the

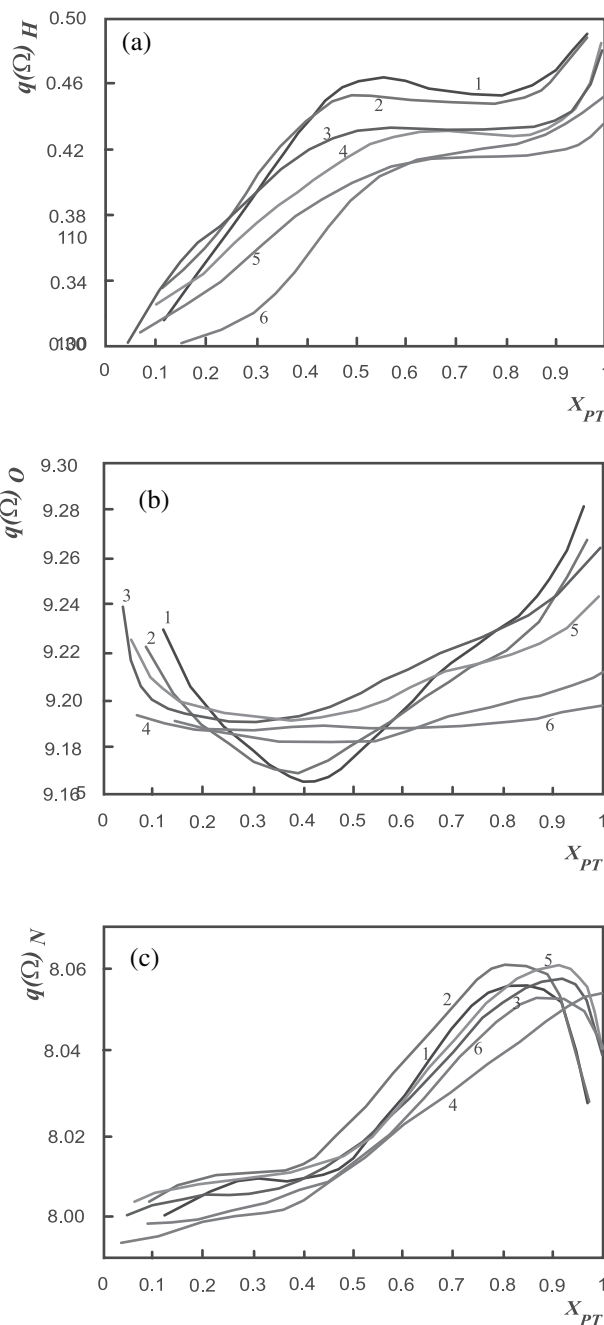


Figure 6. Relationship between the electron density over the atomic volume integrated within the 0.001 isosurface of the atoms participating in the hydrogen bridge: H (a), O (b), and N (c), and proton-transfer degree. The values for H, O in free phenols and O[−] in the phenolate anions are respectively: phenol, 0.4096, 9.1004, 9.2442; 4-nitrophenol, 0.3987, 9.0999, 9.1648; 2,6-dichlorophenol, 0.3923, 9.1111, 9.2138; 2,6-dichloro-4-nitrophenol, 0.3848, 9.1102, 9.1728; 2,4-dinitrophenol, 0.3466, 9.1390, 9.1547; and picric acid 0.3432, 9.1225, 9.1305. The electron densities over the atomic volumes of the H and N atoms in the trimethylammonium cation are 0.5353 and 7.9992, respectively. This figure is available in colour online at www.interscience.wiley.com/journal/poc

relationship with CO distance. Optimization at the MP2/6-311+G** level gives rise to a slightly different geometry and the results obtained for the phenol complexes cannot be included in the relationship obtained using the B3LYP method.

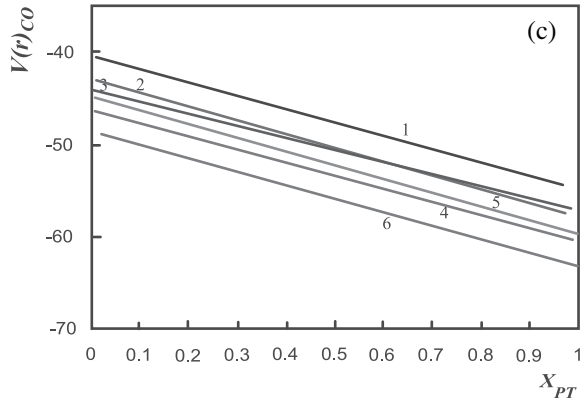
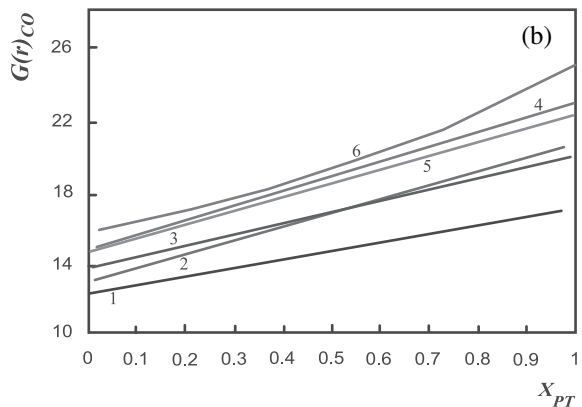
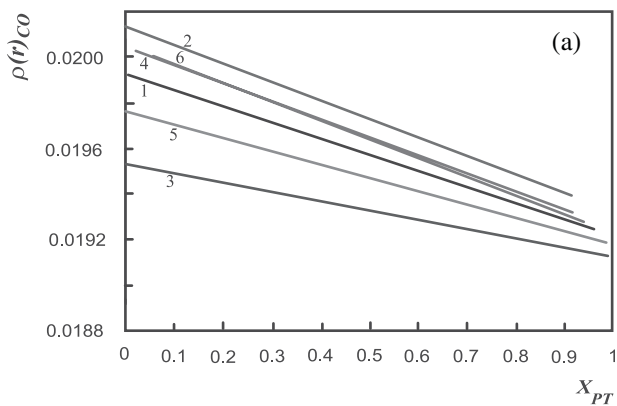


Figure 7. Relationships between the parameters characterizing the BCP of the CO bond in phenols (a) electron density at BCP, (b) kinetic and (c) potential energy density of electrons at BCP and the proton-transfer degree. This figure is available in colour online at www.interscience.wiley.com/journal/poc

Analysis of the phenol RCP

The AIM parameters of RCP of phenol are collected in Table 3 (Supplementary Materials). Compared with the electron density at the BCP of the CO bond, analogous changes at the RCP are very limited, but a regular change with X_{PT} is seen (Fig. 8). Transfer of the proton in the hydrogen bond causes a change in the electron cloud in the aromatic ring of the proton donor molecule. The relationships of electron density and potential energy density are linear and show decreasing values with shifting of the proton from the donor to the acceptor. The kinetic energy density of the

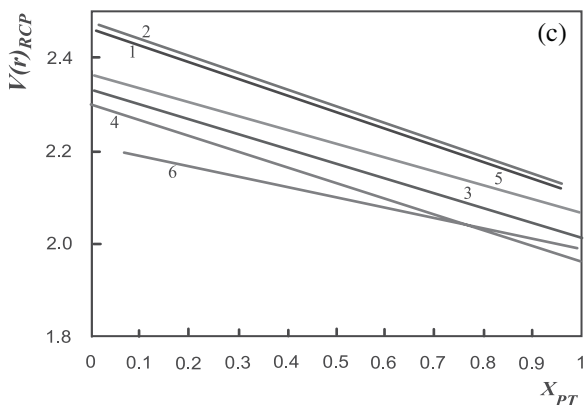
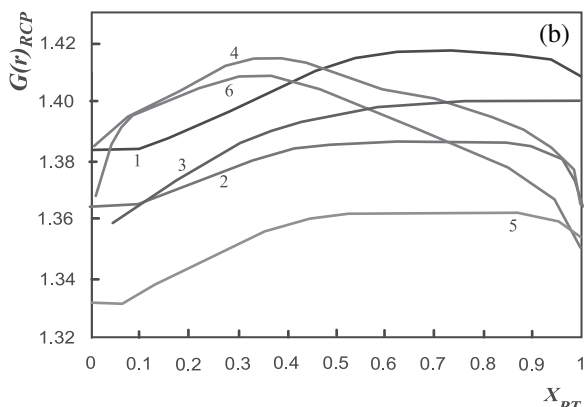
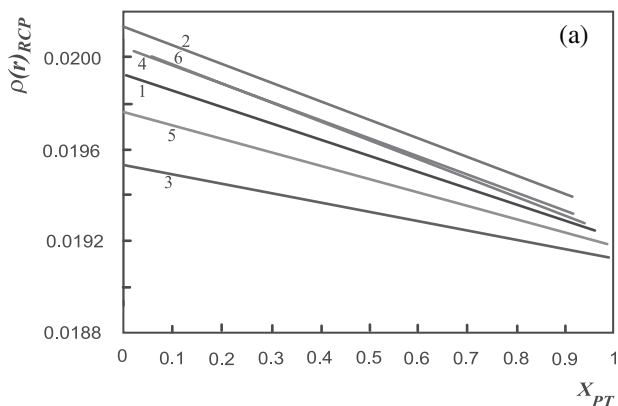


Figure 8. Relationship between the parameters characterizing the RCP of the phenol ring (a) electron density at RCP, (b) kinetic, and (c) potential energy density of electrons at RCP and the proton-transfer degree. This figure is available in colour online at www.interscience.wiley.com/journal/poc

electrons at the RCP changes in a more complicated way and the relationship with X_{PT} has a parabolic shape with a maximum at about 0.5. When the proton is shifted by 50%, the electrons in the aromatic ring of the proton donor molecule are most mobile. The previously analyzed electron density in the atomic basin of the oxygen atom decreases with the proton transfer, which is connected with the movement of the electrons to the NH bond. At about 0.5 the electron density in the oxygen basin reaches a minimum, and for higher X_{PT} values it increases. This is connected with the shifting of the electron cloud from the CO bond and also with the shifting of the electrons from the aromatic ring of the

proton donor. In all the relationships for the RCP, differences between the phenols are seen, but the differences are not directly related to the proton donor properties of the phenol.

Despite the limited changes in electron density at the RCP of the phenol ring, it was interesting to investigate whether these changes are connected with changes in the bonds which are sensitive to the shifting of the proton in the hydrogen bond. The relationship of the electron density at the BCPs of the CO bond with the electron density at the phenol RCP (Supplementary Materials) shows that the CO bond, despite the small range of change in electron density, can be used as a measure of the strength of the hydrogen bond. The differences between phenols are seen in the continuous changes in the electron densities of the OH and NH bonds, so the CO bond can be useful for investigating the differences between proton donors. The relationships of the electron density of the BCP of the CO bond are linear and express the fact that with the shifting of the proton to the acceptor, electrons shift from the phenol ring to the CO bond. The relationships of the electron density of the O···H and N···H bonds with that at the phenol ring are more complicated and illustrate the mechanism of the shifting of the electron cloud during proton transfer. Electrons are shifted not only from the O···H to the N···H bond, but also from the CO bond. Additionally, when the proton-transfer degree is above 0.5, electrons from the aromatic ring of the proton donor are delivered to the hydrogen bridges what is connected with increase in the mobility of electrons at the phenol RCP.

All hydrogen bonds can be classified as charge-assisted hydrogen bonds and resonance-assisted hydrogen bonds.^[46] The latter are typical for very strong bonds in which the hydrogen bond strength is increased by significant delocalization of the π electrons in the vicinity of the hydrogen bond. Delocalization of the π electron is especially easy to realize not only in intramolecular hydrogen bonds in which the six-member ring favors delocalization of the electrons, but also intermolecular N—H···O can be assisted by resonance.^[47] Classification of the very strong OHN hydrogen bond in phenol–amine complexes is not easy. It is rather an example of a CAHB,^[48,49] but anyway a strengthening of the hydrogen bond is always accompanied by a shift of the electron density from the proton donor aromatic ring to the acceptor. The investigation of the electron density performed in this study shows how the delocalization of the electrons in proton donor changes under different degrees of proton transfer and confirms that even for the strongest hydrogen bond it is far from the resonance.

CONCLUSIONS

1. Shifting the proton from donor to acceptor also causes changes in electron density in the part of the molecule not closely connected to the bridge atoms.
2. The changes in electron density in the proton-transfer process are highest for the O···H bond. AIM parameters of the N···H bond change are about three times lower. Because both these bonds are similarly rearranged in the proton-transfer process, these values are specific for the bond type.
3. When the proton-transfer degree is 0.5, the electron density, its Laplacian, the mobility of the electrons, and the potential energy density of the electrons are equal at the BCPs of O···H and N···H. The kinetic energy density of the electrons at the phenol RCP is at a maximum.

4. The relationships of the AIM parameters do not follow a common line, but are different for different proton donors, reflecting their pK_a values. This is especially seen for the CO bond, which can be used as an illustration of specific properties of proton donors.
5. The AIM parameters characterizing the phenolate anion cannot be included in the relationships characterizing phenols participating in the hydrogen bond. The values for phenols can be included in the relationships of the AIM parameters of the CO BCP and the phenol RCP, but the values of the phenolate anion are significantly different. This difference underlines the fact that the formation of the hydrogen bond complex changes the electron density of the OH bond when the transfer of the proton to the acceptor results in a phenolate anion with electron density similar to neither phenol nor a hydrogen-bonded complex.
6. Some relationships as $\rho(r)_{O\cdots H}$, $\rho(r)_{H\cdots N}$, $G(r)_{O\cdots H}$, $G(r)_{H\cdots N}$, $V(\Omega)_{H}$, $q(\Omega)_{H}$, and $q(\Omega)_{N}$ on X_{PT} have shapes similar to the sigmoidal relationships characteristic for many experimental dependencies.

Acknowledgements

The Wroclaw Center for Networking and Supercomputing is acknowledged for generous computer time.

REFERENCES

- [1] I. Majerz, Z. Malarski, L. Sobczyk, *Chem. Phys. Lett.* **1997**, *274*, 361–364. and the papers cited therein.
- [2] I. Majerz, A. Koll, *Acta Crystallogr. B* **2004**, *B60*, 406–415.
- [3] E. Kwiatkowska, I. Majerz, A. Koll, *Chem. Phys. Lett.* **2004**, *398*, 130–139.
- [4] I. Majerz, E. Kwiatkowska, A. Koll, *J. Phys. Org. Chem.* **2005**, *18*, 833–843.
- [5] I. Olovson, G. Jonsson, in *The Hydrogen Bond. Recent Developments in Theory and Experiments*, Vol. II (Eds.: P. Schuster, G. Zundel, C. Sandorfy) North-Holland, Amsterdam, **1976**, 393–455.
- [6] T. Steiner, *J. Phys. Chem. A* **1998**, *102*, 7041–7052.
- [7] T. Steiner, W. Saenger, *Acta Crystallogr. B* **1994**, *50*, 348–357.
- [8] H. Ratajczak, L. Sobczyk, *J. Chem. Phys.* **1969**, *50*, 556–557.
- [9] J. P. Hawranek, L. Sobczyk, *Acta Phys. Pol. A* **1971**, *39*, 651–660.
- [10] P. Huyskens, W. Cleuren, H. M. Van Brabant-Gevaerts, M. A. Vuylsteke, *J. Phys. Chem.* **1980**, *84*, 2740–2748.
- [11] M. Ilczyszyn, H. Ratajczak, K. Skowronek, *Magn. Reson. Chem.* **1989**, *26*, 445–448.
- [12] M. Szafran, B. Brycki, Z. Dega-Szafran, B. Nowak-Wydra, *J. Chem. Soc. Perkin Trans. 2* **1991**, 1161–1166.
- [13] B. Nogaj, E. Dulewicz, B. Brycki, A. Hrynio, P. Barczynski, Z. Dega-Szafran, M. Szafran, P. Koziol, A. R. Katritzky, *J. Phys. Chem.* **1990**, *94*, 1279–1285.
- [14] E. Grech, J. Kalenik, L. Sobczyk, *J. Chem. Soc., Faraday Trans. 1* **1979**, *75*, 1587–1592.
- [15] E. Grech, J. Kalenik, Z. Malarski, L. Sobczyk, *J. Chem. Soc., Faraday Trans. 1* **1983**, *79*, 2005–2012.
- [16] J. Kalenik, I. Majerz, Z. Malarski, L. Sobczyk, *Chem. Phys. Lett.* **1990**, *165*, 15–18.
- [17] M. Rospenk, Z. Malarski, L. Sobczyk, E. Grech, *J. Phys. Chem.* **1982**, *86*, 401–406.
- [18] A. Rabold, G. Zundel, *J. Phys. Chem.* **1995**, *99*, 12158–12163.
- [19] R. Wolny, A. Koll, L. Sobczyk, *Bull. Soc. Chim. Belg.* **1984**, *93*, 99–105.
- [20] I. Majerz, L. Sobczyk, *J. Chim. Phys.* **1993**, *90*, 1657–1666.
- [21] R. F. W. Bader, *Atoms in Molecules: A Quantum Theory*, Oxford University Press, New York, 1990.
- [22] I. Alkorta, J. Elguero, *J. Phys. Chem. A* **1999**, *103*, 272–279.

[23] M. V. Vener, A. V. Mannaev, A. N. Egorova, V. G. Tsirelson, *J. Phys. Chem. A* **2007**, *111*, 1155–1162.

[24] L. F. Pachos, O. Galvez, P. C. Gomez, *J. Chem. Phys.* **2005**, *122*, 214307–214318.

[25] S. J. Grabowski, W. A. Sokalski, J. Leszczyński, *J. Phys. Chem. A* **2006**, *110*, 4772–4779.

[26] A. Kovacs, I. Macsar, I. Hargittai, *J. Phys. Chem. A* **1999**, *103*, 3110–3114.

[27] H. Lampert, W. Mikenda, A. Karpfen, *J. Phys. Chem. A* **1997**, *101*, 2254–2263.

[28] Gaussian 03, Revision A.9, Gaussian, Inc. (2004), Pittsburgh PA.

[29] F. Biegler-König, J. Schönbohm, D. Bayles, *J. Comput. Chem.* **2001**, *22*, 545–559.

[30] I. Majerz, E. Kwiatkowska, A. Koll, *J. Mol. Struct.* **2007**, *831*, 106–113.

[31] P. Huyskens, Th. Zeegers-Huyskens, *J. Chim. Phys.* **1964**, *61*, 81–86.

[32] U. Koch, P. L. A. Popelier, *J. Phys. Chem. A* **1995**, *99*, 9747–9754.

[33] E. Espinosa, I. Alkorta, J. Elguero, E. Molins, *J. Chem. Phys.* **2002**, *117*, 5529–5542.

[34] Yu. A. Abramov, *Acta Crystallogr. A* **1997**, *53*, 264–272.

[35] E. Espinosa, E. Molins, C. Lecomte, *Chem. Phys. Lett.* **1998**, *285*, 170–173.

[36] E. Espinosa, I. Alkorta, I. Rozas, J. Elguero, E. Molins, *Chem. Phys. Lett.* **2001**, *336*, 457–461.

[37] E. Espinosa, C. Lecomte, E. Molins, *Chem. Phys. Lett.* **1999**, *300*, 745–748.

[38] T. Pedersen, N. W. Larsen, L. Nygard, *J. Mol. Struct.* **1969**, *4*, 59–64.

[39] T. Sakurai, *Acta Crys.* **1962**, *15*, 1164–1173.

[40] M. Perrin, P. Michel, *Acta Crystallogr. B* **1973**, *29*, 253–258.

[41] T. Kagawa, R. Kawai, S. Kashino, M. Haisa, *Acta Crystallogr. B* **1976**, *32*, 3171–3175.

[42] F. Iwasaki, Y. Kawano, *Acta Crystallogr. B* **1977**, *33*, 2455–2459.

[43] K. Maartman-Moe, *Acta Crystallogr. B* **1969**, *25*, 1452–1460.

[44] I. Van Bellingen, G. Germain, P. Piret, M. Van Meersche, *Acta Crystallogr. B* **1971**, *27*, 560–564.

[45] A. N. Talukdar, B. Chandhuri, *Acta Crystallogr. B* **1976**, *25*, 803–808.

[46] P. Gilli, V. Bertolasi, V. Ferretti, G. Gilli, *J. Am. Chem. Soc.* **1994**, *116*, 909–915.

[47] V. Bertolasi, P. Gilli, V. Ferretti, G. Gilli, *Acta Crystallogr. B* **1995**, *51*, 1004–1015.

[48] P. Gilli, V. Bertolasi, L. Pretto, A. Lycka, G. Gilli, *J. Am. Chem. Soc.* **2002**, *124*, 13554–13567.

[49] P. Gilli, V. Bertolasi, L. Pretto, V. Ferretti, G. Gilli, *J. Am. Chem. Soc.* **2004**, *126*, 3845–3855.